Available online at www.sciencedirect.com
SCIENCE DIRECT®
Composites: Part B 35 (2004) 523–534
composites Part B: engineering
www.elsevier.com/locate/compositesb

Collapse of clamped and simply supported composite sandwich beams in three-point bending

V.L. Tagarielli, N.A. Fleck*, V.S. Deshpande

Department of Cambridge University Engineering, University of Cambridge, Trumpington Street, Cambridge CB2 1PZ, UK

Received 6 June 2003; accepted 28 July 2003

Available online 16 April 2004

Abstract

Composite sandwich beams, comprising glass–vinylester face sheets and a PVC foam core, have been manufactured and tested quasi-statically. Clamped and simply supported beams were tested in three-point bending in order to investigate the initial collapse modes, the mechanisms that govern the post-yield deformation and parameters that set the ultimate strength of these beams. Initial collapse is by three competing mechanisms: face microbuckling, core shear and indentation. Simple formulae for the initial collapse loads of clamped and simply supported beams along with analytical expressions for the finite deflection behaviour of clamped beams are presented. The simply supported beams display a softening post-yield response, while the clamped beams exhibit hardening behaviour due to membrane stretching of the face sheets. Good agreement is found between the measured, analytical and finite element predictions of the load versus deflection response of the simply supported and clamped beams. Collapse mechanism maps with contours of initial collapse load and energy absorption are plotted. These maps are used to determine the minimum mass designs of sandwich beams comprising woven glass face sheets and a PVC foam core.
© 2004 Elsevier Ltd. All rights reserved.

Keywords: A. Polymer-matrix composites; C. Finite element analysis; C. Analytical modelling; D. Mechanical testing; Sandwich beam optimisation

1. Introduction

Sandwich beams comprising stiff and strong face sheets and a low density core, are commonly used for weight efficient structures subject to bending loads. However, sandwich beams are susceptible to unconventional failure modes such as core shear and face sheet wrinkling—see Refs. [1,2] for discussions on the collapse of metallic and composite sandwich beams, respectively.

Composite sandwich beams comprising composite face sheets and a polymer foam core are extensively used in lightweight marine applications. Steeves and Fleck [3,4] have investigated the three-point bending response of simply supported sandwich beams made from glass–epoxy face sheets and a polymer foam core. They developed an initial collapse map which relates the collapse mechanism and strength of the beams to the properties of the constituent materials and to the structural geometry. In many practical applications, sandwich beams are attached to stiff metal structures (e.g. ship frame), and hence the rotation and pull-in of the beam ends is largely restrained. Clamped rather than simply supported boundary conditions are expected to model such beams more realistically.

This study focuses on the effect of simply supported and clamped boundary conditions on the load versus deflection response of beams loaded in three-point bend. First, analytical formulae are developed for the elastic stiffness and initial collapse strength of composite beams. The post-yield response of clamped beams is also modelled by employing a membrane assumption. Next, an experimental investigation of sandwich beams comprising woven glass face sheets and a PVC foam core is described: clamped and simply supported beams were tested in three-point bending and their load versus deflection response is contrasted. Comparisons between experimental measurements and analytical and finite element (FE) predictions are presented. Finally, the analytical formulae developed for the initial collapse and energy absorption capacity of the clamped beams are used to determine optimal designs that minimise the mass of such beams subject to a constraint on the initial collapse load or energy absorption capacity.

* Corresponding author. Tel.: +44-1223-332650; fax: +44-1223-765046.
E-mail address: naf1@eng.cam.ac.uk (N.A. Fleck).

1359-8368/$ - see front matter © 2004 Elsevier Ltd. All rights reserved.
doi:10.1016/j.compositesb.2003.07.001

2. Analytical modelling of the load–deflection response

In this section, we summarise simple formulae for the stiffness and collapse strength of simply supported and clamped sandwich beams. Consider a sandwich beam of length l and uniform width b, comprising two identical face-sheets of thickness t, bonded to a foam core of thickness c, as sketched in Fig. 1. The beam is loaded centrally by a force P via a roller of radius R. In the simply supported case the supporting rig reacts with only vertical forces $P/2$, while in the clamped case the supports also provide resisting bending moments and an axial force. The analysis developed below pertains to composite sandwich beams comprising a polymer foam core and composite face sheets. Hence, we shall assume that the face sheets are elastic-brittle with a Young's modulus E_f and microbuckling strength σ_f, while the core is modelled as an elastic ideally plastic solid with axial and shear moduli E_c and G_c, and compressive and shear strengths σ_c and τ_c.

2.1. Analytical formulae for stiffness of sandwich beams

The relative elastic deflection δ of the roller with respect to the supports is the sum of the flexural and shear deflections. For simply supported beams δ is given by [5]

$$\delta = \frac{Pl^3}{48EI_{eq}} + \frac{Pl}{4AG_{eq}}, \tag{2.1}$$

where

$$EI_{eq} = \frac{E_f btd^2}{2} + \frac{E_f bt^3}{6} + \frac{E_c bc^3}{12} \approx \frac{E_f btd^2}{2}, \tag{2.2}$$

and

$$AG_{eq} = \frac{bd^2}{c} G_c \approx bcG_c. \tag{2.3}$$

Here, E_c and G_c are Young's modulus and shear modulus, respectively, of the core material and $d = c + t$. For the clamped beams, the shear deflections remain the same while the flexural deflections decrease, and the elastic load versus deflection relation is given by

$$\delta = \frac{Pl^3}{384EI_{eq}} + \frac{Pl}{4AG_{eq}}. \tag{2.4}$$

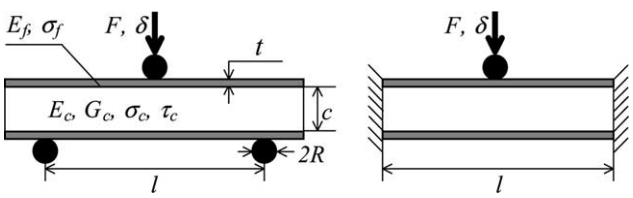

Fig. 1. Geometries of the simply supported and clamped sandwich beams.

2.2. Initial collapse of simply supported beams

The initial collapse modes for simply supported composite sandwich beams have been investigated by Steeves and Fleck [3]; here we summarise their results. Three possible collapse mechanisms have been identified for sandwich beams with composite faces and a polymer foam core: face microbuckling, core shear and indentation beneath the loading roller, as shown in Fig. 2. The active collapse mechanism is the one associated with the lowest collapse load for a given set of material properties and geometrical parameters.

2.2.1. Face microbuckling

The sandwich beam fails by microbuckling of the upper face sheet when the compressive stress in this face attains the characteristic microbuckling strength σ_f. Upon neglecting the core contribution to the bending strength, moment equilibrium across the central section of the sandwich beam dictates that the collapse force P_{fm}^{ss} to activate this mechanism is

$$P_{fm}^{ss} = \frac{4dbt\sigma_f}{l}. \tag{2.5}$$

The superscript 'ss' refers to simply supported, while the subscript 'fm' refers to 'face microbuckling'.

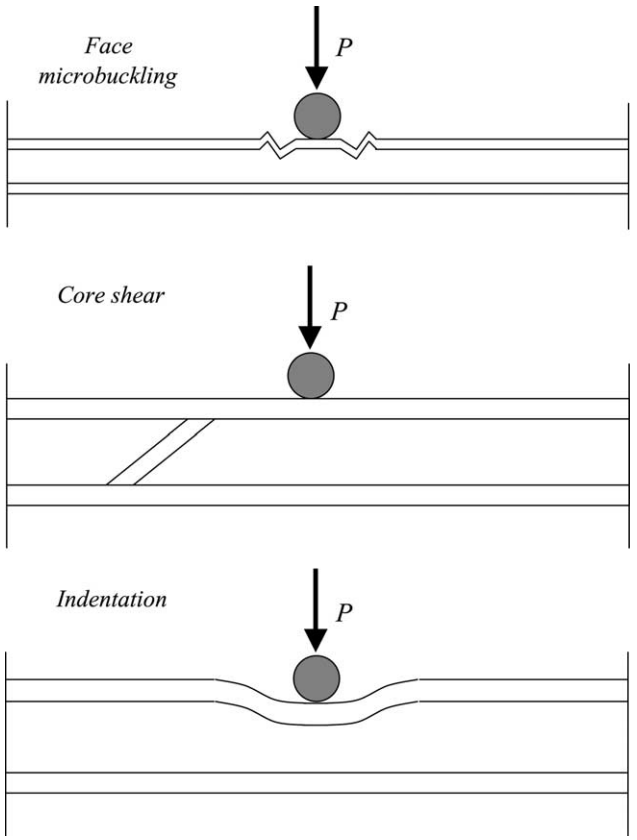

Fig. 2. Competing failure modes of simply supported or clamped sandwich beams subjected to three-point bending.

2.2.2. Core shear

For sandwich beams with relatively thin faces compared with that of the core, it may be assumed that the core material collapses at a uniform shear strength τ_c, with negligible additional strength from the composite faces. With this approximation, the load P_{cs}^{ss} required to initiate the core shear mechanism is given by

$$P_{cs}^{ss} = 2bd\tau_c. \tag{2.6}$$

2.2.3. Indentation

A simple model to describe the indentation of a sandwich beam by means of a concentrated force has been developed by Steeves and Fleck [3]. They assumed that the face sheets remain elastic during the indentation event, and that the core can be treated as a rigid perfectly plastic solid. Thus, as sketched in Fig. 3, the upper face sheet is modelled as an elastic beam-column upon a rigid perfectly plastic foundation. The face sheet is loaded by a transverse force P and by an axial force F, as dictated by moment equilibrium. Steeves and Fleck [3] thereby showed that the maximum load P_{in}^{ss} that the beam can withstand is given by

$$P_{in}^{ss} = bt\left(\frac{\pi^2\, dE_f\sigma_c^2}{3l}\right)^{1/3}. \tag{2.7}$$

2.3. Initial collapse of clamped beams

The experimental investigation reported below reveals that the initial collapse mechanisms are similar for clamped and simply supported sandwich beams. However, the magnitude of the collapse loads for the clamped beams differ from those detailed above for the simply supported case due to differences in bending moment distribution. In the following sub-sections, we review the three collapse mechanisms of clamped beams and calculate the associated collapse loads.

2.3.1. Face microbuckling

It is anticipated that clamped sandwich beams fail by microbuckling of the face sheets when the compressive stress in this face attains the characteristic microbuckling strength σ_f. Upon neglecting the contribution of the core to the bending strength, moment equilibrium across the section of the sandwich beam at the location of maximum bending moment implies that the collapse force P_{fm}^{cl} to activate this mechanism is

$$P_{fm}^{cl} = \frac{8bdt}{l}\sigma_f. \tag{2.8}$$

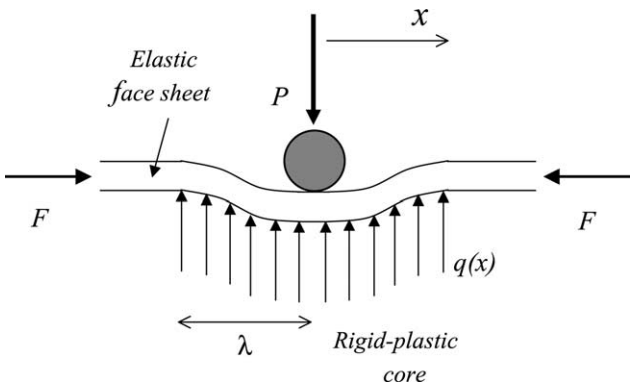

Fig. 3. Sketch of the indentation collapse of the upper face sheet.

2.3.2. Core shear

As for the simply supported case, the core shear collapse load P_{cs}^{cl} is determined by neglecting the contribution from the faces; thus, Eq. (2.6) provides

$$P_{cs}^{cl} = P_{cs}^{ss} = 2bd\tau_c. \tag{2.9}$$

2.3.3. Indentation

We develop a model for the indentation of a clamped sandwich beam following the approach proposed by Steeves and Fleck [3]. It is worth emphasising that the analysis is based on a small deflection hypothesis and therefore the load versus deflection relation derived is expected to be valid only in the early stages of deformation.

Consider a clamped sandwich beam in three-point bending as sketched in Fig. 3. As mentioned above, we assume that the face sheets are elastic and the core is a rigid perfectly plastic solid. The transverse load P at mid-span induces a bending moment $M = Pl/8$ in the central section. Assuming that this moment is carried only by the face sheets, equilibrium dictates that the upper face sheet is subjected to a compressive force

$$F = \frac{M}{d} = \frac{Pl}{8d}. \tag{2.10}$$

In the indentation zone of length 2λ, the core is compressed and will exert a force per unit of length $q = \sigma_C b$ on the upper face sheet. Now consider a typical element of the elastic face sheet subject to a transverse load q per unit length and to an axial force F. With $u(x)$ as the transverse deflection of the beam element, equilibrium dictates that

$$q = \frac{dV}{dx}, \tag{2.11}$$

and

$$F\frac{du}{dx} + V = \frac{dM}{dx}. \tag{2.12}$$

Here, x is the axial co-ordinate measured from the beam centre as sketched in Fig. 3, and V and M are the shear force and bending moment, respectively. Using classical beam theory, the bending moment is related to the curvature by

$$M = -E_f I_f \frac{d^2u}{dx^2}, \tag{2.13}$$

where

$$I_f = \frac{bt^3}{12}. \tag{2.14}$$

Combining Eqs. (2.11)–(2.13), the governing equation for the upper face sheet is given by

$$\frac{d^4u}{dx^4} + \frac{F}{E_f I_f}\frac{d^2u}{dx^2} = -\frac{\sigma_C b}{E_f I_f}. \tag{2.15}$$

This differential equation admits a general solution of the form

$$u(x) = A_1\cos(kx) + A_2\sin(kx) + A_3x + A_4 - \frac{\sigma_C b x^2}{2F}, \tag{2.16}$$

where

$$k = \sqrt{\frac{F}{E_f I_f}}, \tag{2.17}$$

and A_i are four constants. The five unknowns A_1, A_2, A_3, A_4 and the indentation zone length λ are obtained from the following boundary conditions:

(i) Symmetry about the central line dictates that

$$u'(0) = 0. \tag{2.18}$$

(ii) The shear force at $x = 0$ is $P/2$ which implies

$$u'''(0) = \frac{P}{2E_f I_f}. \tag{2.19}$$

(iii) The core is uncompressed outside the indentation zone and thus

$$u(\lambda) = 0. \tag{2.20}$$

(iv) Since the beam remains elastic, the bending moment and slope of the beam at the edge of the indentation zone, $x = \lambda$, are zero which gives

$$u''(\lambda) = 0, \tag{2.21}$$

and

$$u'(\lambda) = 0, \tag{2.22}$$

respectively.

With $k = \mu\lambda$ the boundary conditions (2.18)–(2.22) give the constants A_i as

$$A_1 = \frac{4d}{kl}\left(\frac{1-\cos\mu-\mu\sin\mu}{\sin\mu-\mu\cos\mu}\right), \tag{2.23}$$

$$A_2 = -\frac{4d}{kl}, \tag{2.24}$$

$$A_3 = \frac{4d}{l}, \tag{2.25}$$

and

$$A_4 = \frac{4d}{kl}\left(\frac{1-\cos\mu-\mu\sin\mu}{\sin\mu-\mu\cos\mu}\right) + \frac{2d\mu^2}{kl}\left(\frac{1+\cos\mu}{\sin\mu-\mu\cos\mu}\right), \tag{2.26}$$

and specify the load P to be

$$P = bt\left(\frac{8\,dE_f\sigma_C^2}{3l}\left(\frac{\sin\mu-\mu\cos\mu}{1-\cos\mu}\right)\right)^{1/3}. \tag{2.27}$$

Eliminating k from the above equations we get

$$\lambda = \mu t\left(\frac{dE_f}{3l\sigma_C}\left(\frac{1-\cos\mu}{\sin\mu-\mu\cos\mu}\right)\right)^{1/3}, \tag{2.28}$$

while the displacement $u(0)$ of the loading roller is given by

$$u(0) = A_1 + A_4 = \frac{8d}{kl}\left(\frac{1-\cos\mu-\mu\sin\mu}{\sin\mu-\mu\cos\mu}\right) + \frac{2d\mu^2}{kl}\left(\frac{1+\cos\mu}{\sin\mu-\mu\cos\mu}\right). \tag{2.29}$$

Eqs. (2.27)–(2.29) give the load, deflection and indentation wavelength, respectively, as functions of the parameter μ. It can be shown that the function $u(\mu)$ is monotonic in μ, and its derivative is always positive. Hence, a peak in $P(u_{x=0})$ corresponds to a peak in $P(\mu)$. By setting $dP/d\mu$ equal to zero, we find that the maximum load is given by

$$P_{max} = bt\left(\frac{2\pi^2\,dE_f\sigma_C^2}{3l}\right)^{1/3}, \tag{2.30}$$

at $\mu = \pi$. The deflection at $x = 0$ and indentation wavelength corresponding to this maximum load P_{max} are given by

$$u_{P\,max} = 16t\left(\frac{d}{l\pi}\right)^{4/3}\left(\frac{2E_f}{3\sigma_C}\right)^{1/3}, \tag{2.31}$$

and

$$\lambda_{P\,max} = t\left(\frac{2\pi^2\,dE_f}{3l\sigma_C}\right)^{1/3}, \tag{2.32}$$

respectively. P_{max} is the maximum load that the beam can sustain for this collapse mechanism and we take it to be the value of the applied load that initiates the indentation collapse mechanism in clamped sandwich beams.

2.4. Large deflection of clamped beams

The maximum load carrying capacity of simply supported beams is given by the initial collapse loads as detailed in Section 2.2. In contrast, clamped beams can undergo membrane stretching of the face-sheets beyond

initial yield which gives rise to a hardening post-yield response. We analyse the post-yield response of clamped beams in this section. It is worth emphasising here that if face microbuckling is the initial collapse mode, the microbuckled top face has negligible tensile strength; consequently, the following analysis is inapplicable. However, it is shown subsequently that the face microbuckling mode is not likely to occur for most practical designs of the composite beams considered here and hence it is reasonable to neglect this possibility.

A straightforward estimate of the finite deflection profile for the sandwich beam is obtained by neglecting the bending stiffness of the beam. Then, the deflection profile of the beam can be taken to be triangular in shape, as sketched in Fig. 4, with the beam rotating through an angle θ at the supports. Upon taking the deflection δ of the centre of the beam to be small compared to the beam length l, the change in length Δl of the beam is

$$\Delta l \approx \frac{2\delta^2}{l}, \tag{2.33}$$

and hence the average axial strain along the beam is

$$\varepsilon(\delta) = \frac{2\delta^2}{l^2}. \tag{2.34}$$

The composite face sheets are assumed to be elastic-brittle solids. Hence, the membrane force N due to the axial straining (neglecting core contribution) is given by

$$N = 4E_f tb\frac{\delta^2}{l^2}, \tag{2.35}$$

and vertical equilibrium dictates that

$$P \approx 2N\theta = \frac{4N\delta}{l} = 16E_f tb\left(\frac{\delta}{l}\right)^3. \tag{2.36}$$

It is difficult to state a precise failure criterion for the beam as the load for incipient failure is sensitive to the details of the built-in end conditions. Here, we state a failure criterion based on an estimate of the tensile strain in the face sheets due to stretching of the beam and neglect the tensile strain due to bending. For an assumed ductility ε_f of the face sheet material, the deflection δ_f at failure is given by setting $\varepsilon = \varepsilon_f$ in Eq. (2.34) and thus

$$\delta_f = l\sqrt{\frac{\varepsilon_f}{2}}, \tag{2.37}$$

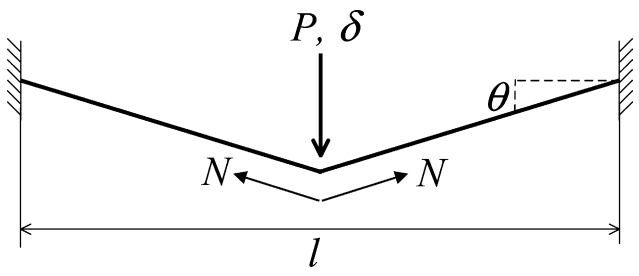

Fig. 4. Sketch of membrane idealisation of sandwich beams.

with the corresponding failure load P_f given by

$$P_f = 16btE_f\left(\frac{\varepsilon_f}{2}\right)^{3/2}. \tag{2.38}$$

In summary, the load versus deflection response of clamped beams may be divided into three phases as sketched in Fig. 5:

(i) *Elastic bending*. The beam deflects elastically until the value of the initial collapse load P_c associated with the operative collapse mechanism is reached. The load P_c is attained at an elastic deflection δ_e as dictated by Eq. (2.4).
(ii) *Transition phase*. In this phase, we assume that the beam deforms at a constant load, equal to the initial collapse load P_c. This phase ends at a value of the deflection δ_T at which the membrane load (2.36) equals the initial collapse load P_c.
(iii) *Membrane phase*. The beam behaves as a stretched elastic string and the load versus deflection response is given by Eq. (2.36); the sandwich beam deflects until there is a sudden loss of load carrying capacity due to face sheet tearing at the failure load P_f.

The energy absorption W is the area under the load versus deflection curve of the sandwich beam. Upon neglecting the energy absorption in the elastic bending phase, W is given by

$$W = P_c\delta_T + \frac{4btE_f}{l^3}(\delta_f^4 - \delta_T^4), \tag{2.39}$$

where

$$\delta_T = l\left(\frac{P_c}{16E_f tb}\right)^{1/3}, \tag{2.40}$$

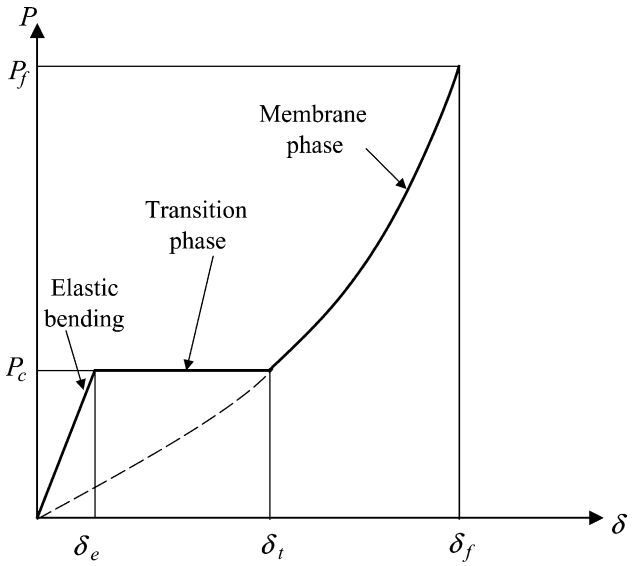

Fig. 5. Sketch of the three phases of the load versus deflection response of clamped sandwich beams.

and δ_f has already been specified by Eq. (2.37). Here, P_c is the load associated with the operative initial collapse mechanism.

3. Experimental investigation

Clamped and simply supported beams comprising a PVC foam core and woven glass face sheets were tested in three point bending in order to explore the pertinence of the theory outlined above. In this section, we describe this experimental investigation.

3.1. Materials

The sandwich beams tested were manufactured at *KTH*[1] by a vacuum infusion technique that allowed for the infusion of the face sheets and their assembly with the core in a single step, under the action of atmospheric pressure. The 0.9 mm thick woven glass face sheets comprised a quasi-isotropic glass fibre fabric DBLT850 (with equal amounts of fibres in the 0, + 45, 90 and − 45° directions) infused with a vinylester resin, giving a composite density of 1700 kg/m^3. H100 Divinycell PVC foam (density 100 kg/m^3) was employed as the core of the sandwich beams; this combination of materials is commonly used in marine applications. In the present study, 12 specimens with 6 different geometries were manufactured and tested in three-point bending with simply supported and clamped boundary conditions.

3.2. Tests on the constituent materials

In order to determine the mechanical properties of the constituent materials, uniaxial compression and tension tests were conducted on the composite face sheet material and uniaxial compression and shear tests on the foam core material.

In tension, the face sheet material exhibits an initial stiffness of about 10 GPa. At a strain level of approximately 0.5%, matrix cracking initiates which reduces the stiffness to about 7.5 GPa. A linear response continues until the laminate fails by tensile tearing. Six repeat tensile tests were conducted on the woven glass fibre laminate, and gave an average tensile strength of 220 MPa and an associated tensile ductility $\varepsilon_f = 2.5\%$. In compression, the laminate displays a linear response, with a compressive axial modulus slightly less than the tensile modulus due to fibre waviness. The microbuckling compressive strength is approximately 150 MPa and is attained at a compressive strain of about 1.6%.

In uniaxial compression the Divinycell H100 foam core exhibits an initial elastic, plateau and densification regimes of behaviour. The compressive strength of the foam, defined at an offset strain of 0.2% is found to be 1.7 MPa. Unlike the compressive response, shear test results show that the foam exhibits a softening behaviour in shear, and the measured peak shear strength of approximately 1.0 MPa is attained at an engineering shear strain of about 3%.

3.3. Test method for sandwich beams

In order to guide the choice of sandwich beam geometries, a mechanism map for the initial collapse of simply supported and clamped sandwich beams is constructed from the analysis detailed in Section 2. We start by redefining the beam geometry, material properties and collapse load in non-dimensional terms. The non-dimensional face sheet thickness $\bar{t}$ and core thickness $\bar{c}$ are defined by

$$\bar{t} = \frac{t}{c}; \qquad \bar{c} = \frac{c}{l}, \tag{3.1}$$

while the non-dimensional material properties are defined as

$$\bar{\sigma} = \frac{\sigma_C}{\sigma_f}; \qquad \bar{\tau} = \frac{\tau_C}{\sigma_f}; \qquad \text{and} \qquad \bar{E} = \frac{E_f}{\sigma_f}. \tag{3.2}$$

The non-dimensional structural load index $\bar{P}$ is related to the initial collapse load P by

$$\bar{P} = \frac{P}{bl\sigma_f}. \tag{3.3}$$

Expressions for $\bar{P}$ follow directly from the formulae given in Section 2. For simply supported beams $\bar{P}$ is given by

$$\begin{aligned} &\bar{P}^{ss}_{fm} = 4\bar{c}^2\bar{t}(1+\bar{t}); \qquad \bar{P}^{ss}_{cs} = 2\bar{c}\bar{\tau}(1+\bar{t}); \\ &\bar{P}^{ss}_{in} = \left(\frac{\pi^2}{3}\bar{c}^4\bar{t}^3(1+\bar{t})\bar{E}\bar{\sigma}^2\right)^{1/3}, \end{aligned} \tag{3.4}$$

while for the clamped beam $\bar{P}$ is given by

$$\begin{aligned} &\bar{P}^{cl}_{fm} = 8\bar{c}^2\bar{t}(1+\bar{t}); \qquad \bar{P}^{cl}_{cs} = 2\bar{c}\bar{\tau}(1+\bar{t}); \\ &\bar{P}^{cl}_{in} = \left(\frac{2\pi^2}{3}\bar{c}^4\bar{t}^3(1+\bar{t})\bar{E}\bar{\sigma}^2\right)^{1/3}. \end{aligned} \tag{3.5}$$

It is instructive to construct a failure mechanism map for both the simply supported and clamped sandwich beams, with axes given by the non-dimensional geometrical parameters $\bar{c}$ and $\bar{t}$, at selected values of $\bar{\sigma}, \bar{\tau}$ and $\bar{E}$. The map displays the regimes of dominance for each initial collapse mechanism, and an example is shown in Fig. 6 for the choice of material parameters $\bar{\sigma} = 0.01$, $\bar{\tau} = 0.006$ and $\bar{E} = 66.6$, in line with the measured material properties of the woven glass faces and H100 foam core. In the shaded regions of the map the collapse mechanism is expected to be the same for both boundary conditions. It is noted that the map is dominated by the core shear and indentation regimes

[1] KTH (Kungl Tekniska Högskolan) Royal Institute of Technology. Valhallavägen 79, Stockholm, Sweden.

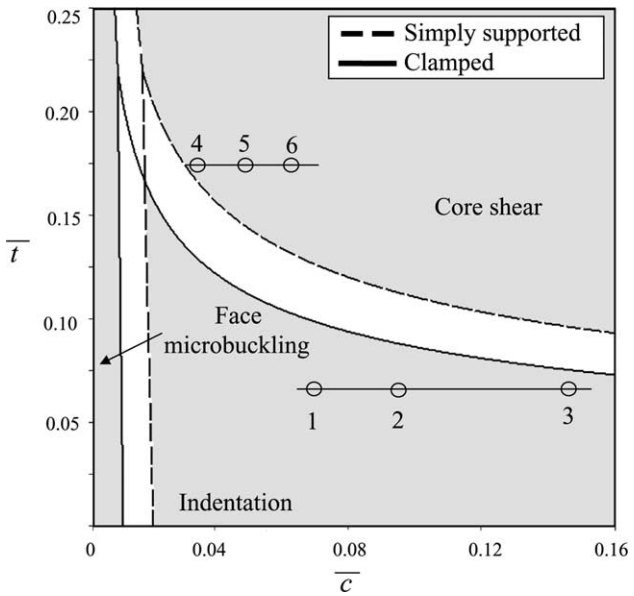

Fig. 6. Initial collapse mechanism map for simply supported and clamped sandwich beams for a material parameters choice $\bar{\sigma} = 0.01$, $\bar{\tau} = 0.006$ and $\bar{E} = 66.6$, which is representative of sandwich beams comprising woven glass face sheets and a H100 PVC foam core. Regimes of dominance of the three collapse mechanisms are marked on the map. The indicated circles represent geometries tested in this study.

with face microbuckling only expected to occur for beams with unrealistically low values of $\bar{c}$.

3.3.1. Test protocol

Sandwich beams of width 35 mm wide have been cut with a diamond grit saw from panels manufactured at *KTH*. The choice of the beam geometries was limited by the fixed thickness of the face sheets (0.9 mm) and by the fact that only two thicknesses of the foam cores (5 and 15 mm) were employed. Furthermore, beam spans had to be kept shorter than 400 mm, due to the limited size of the test rig. Six beam geometries are marked in Fig. 6. These represent the specimens tested in the experimental study, with both simply supported and clamped boundary conditions. The actual dimension of these beams are given in Table 1 with the labelled values in the table corresponding to those marked on Fig. 6. While the specimens with the lowest value of $\bar{t}$ lie in the indentation zone, the other three specimens with a higher $\bar{t}$ are close to the boundary between the indentation and the core shear regime.

Table 1
Designs of the six beams tested in this study

	Specimen no.					
	1	2	3	4	5	6
t, mm	0.9	0.9	0.9	0.9	0.9	0.9
c, mm	15	15	15	5	5	5
l, mm	200	150	100	150	100	80

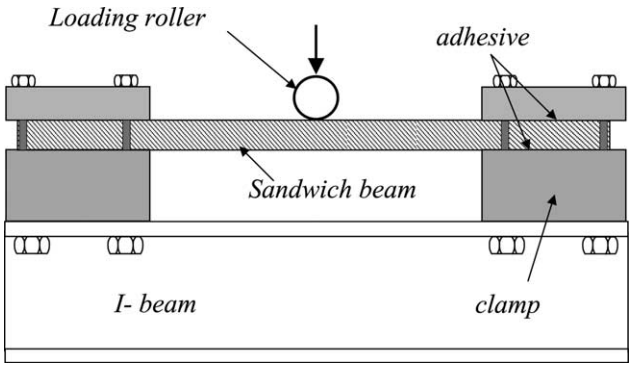

Fig. 7. Sketch of the supporting rig for the three-point bending tests of clamped sandwich beams.

The simply supported sandwich beams were loaded in three-point bending by circular cylindrical rollers of diameter 19 mm. In contrast, the clamped boundary condition was achieved by adhering the beams to a stiff supporting steel structure, as sketched in Fig. 7. For both types of boundary condition, the central roller was displaced at a rate of 0.3 mm s^{-1}. The applied load was measured by the load cell of the test machine and the vertical deflections of top and bottom face sheets were measured by laser extensometers placed at mid-span. In order to gain additional insight into the collapse mechanisms, the beams were instrumented with longitudinal strain gauges at mid-span of the bottom face sheet.

4. Effect of boundary conditions on the sandwich beam response

A comparison of the measured load deflection responses for simply supported and clamped beams of geometry no. 1 is shown in Fig. 8. For both boundary conditions, this beam

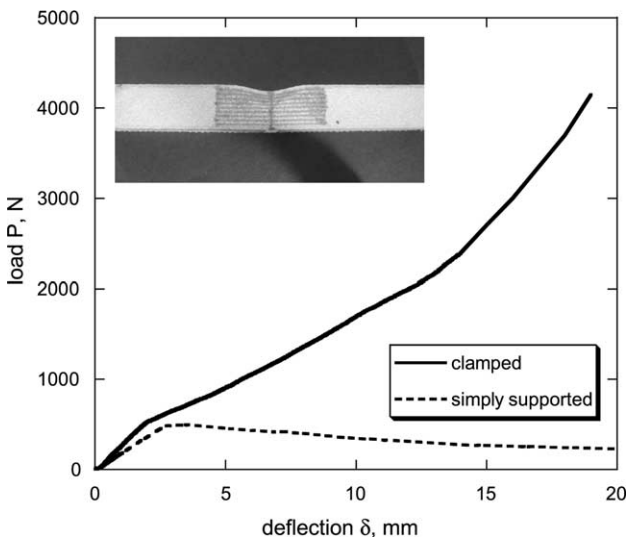

Fig. 8. Effect of boundary conditions on the load versus deflection response of sandwich beams with indentation as the initial collapse mode ($l = 200$ mm, $c = 15$ mm, $t = 0.9$ mm, geometry no. 1).

geometry lies in the indentation regime of the initial collapse mechanism map (Fig. 6) and the indentation mode was indeed observed. The inset in Fig. 8 is a photograph of the clamped beam after the test and clearly shows that the indentation mode was operative; a series of parallel marker lines were placed on the foam core prior to test, and their deflected shape confirms that the indentation is a local event of the top face sheet. A number of differences in the measured load versus deflection response are evident in Fig. 8 for the clamped and simply supported beams:

(i) in the initial linear elastic regime, the clamped beam is stiffer than the simply supported beam;
(ii) the deviation from a linear load versus displacement curve occurs at a higher load for the clamped beam, as anticipated from the analytical formulae; and
(iii) the post-yield response of the simply supported beam is softening while the clamped beam displays a hardening response. In the simply supported case, indentation results in a reduction of core thickness (and consequently a reduction in the 2nd moment of area of the beam cross-section) at mid-span. Thus, the load versus deflection response has a peak. In contrast, in the clamped case, stretching of both face sheets progressively switches off the indentation mechanism and the load increases with continued deflection. This clamped beam test was terminated when the epoxy adhesive failed between the beam and supports.

The measured load versus deflection response of the simply supported beam (geometry no. 4) is shown Fig. 9. Although it is anticipated that this beam collapses by core shear, the observed collapse mode was by a combination of core shear and indentation: a photograph of the deformed beam after the test is given as an inset in Fig. 9. This mixed-mode failure mechanism is consistent with the fact that the beam geometry no. 4 lies near the boundary between the core shear and indentation regimes, with the collapse loads due to both mechanisms approximately equal. Since some indentation occurs in this case, there is a peak in the load versus displacement response similar to that seen in Fig. 8; beyond peak load the load decreases until microbuckling of the upper face sheet occurs with a loss in load carrying capacity of the beam at $\delta \approx 8$ mm. In the clamped case, neither a peak load nor face microbuckling were observed due to stretching of the face sheets, with the beam again displaying a hardening post-yield response. This hardening behaviour continues until the upper face sheet tears at $\delta = 17.2$ mm.

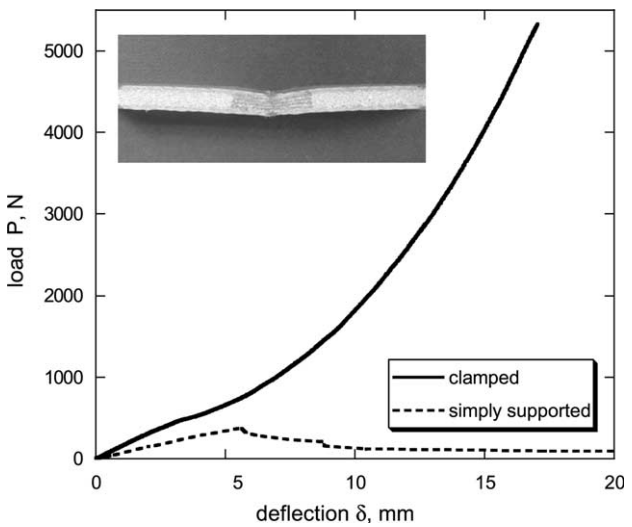

Fig. 9. Effect of boundary conditions on the load versus deflection response of sandwich beams with core shear as the initial collapse mode ($l = 150$ mm, $c = 5$ mm, $t = 0.9$ mm, geometry no. 4).

In summary, experimental measurements of the load versus deflection response of sandwich beams confirmed that the response is strongly influenced by the support boundary conditions, with the clamped beams displaying a hardening post-yield behaviour.

5. Comparison of experiments and predictions

The accuracy of the analytical and FE predictions of the load versus deflection responses of the simply supported and clamped composite sandwich beams is now explored.

5.1. Details of finite element calculations

Finite deformation FE simulations of the simply supported and clamped sandwich beams were performed using the general-purpose FE package ABAQUS. The H100 Divinycell foam core was modelled using the polymer foam constitutive model proposed by Deshpande and Fleck [6] in which the yield surface of the foam is assumed to be quadratic in von-Mises stress σ_e versus mean stress σ_m space and capped by a maximum compressive principal stress criterion. This constitutive model has been implemented as a user defined material law (UMAT) for ABAQUS by Chen and Fleck [7]; a set of shear and uniaxial compression experiments on the H100 Divinycell foam suffice to calibrate the model, as detailed in Steeves and Fleck [4]. The loading was applied through prescribed displacements on a rigid cylindrical roller, with contact between the rollers and the face sheet modelled by a frictionless contact surface as provided by ABAQUS.

While the same foam core model was used for both the simply supported and clamped beams, the face sheets were modelled slightly differently in the two cases. As discussed in Section 4, microbuckling of the face sheets occurred for some of the simply supported beams while tensile straining of the face sheets dominates in the clamped case. To account for this, in the FE simulations of simply supported beams, the face sheet material was modelled as an elastic-perfectly plastic material, with a compressive yield strength equal to

the microbuckling stress $\sigma_f = 150$ MPa: this is aimed to simulate the formation of a hinge at mid-span of the upper face sheet, which first reaches the critical value of the microbuckling stress. On the other hand, for the clamped beams, the face sheet material was assumed to be linear elastic as stretching of the face sheets in this case switches off the microbuckling mode. In both cases, the Young's modulus of the face sheets was taken to be $E_f = 10$ GPa and the Poisson's ratio $\nu = 0.3$. Typical undeformed and deformed meshes are shown in Fig. 10 for three-point loading of clamped sandwich beams; Fig. 10a shows that the initial collapse mode is indentation for geometry no. 1, while Fig. 10b shows that geometry no. 4 undergoes core shear.

5.2. Detailed comparisons

FE simulations (and analytical calculations) have been performed for each geometry under clamped boundary conditions These comparisons are described below. Only limited comparisons are reported here for the simply supported case (geometries 1 and 4) since Steeves and Fleck [4] have already demonstrated that the FE simulations and analytical calculations are accurate in the simply supported case.

Consider first the case of simply supported beams. Fig. 11 provides a comparison of the measured, and analytical and FE predictions of the load versus deflection response for the simply supported beam of geometry no. 1. The collapse mechanism for this beam is indentation. Both the FE and analytical models predict the stiffness and peak load for this beam to a reasonable accuracy. While the finite deformation

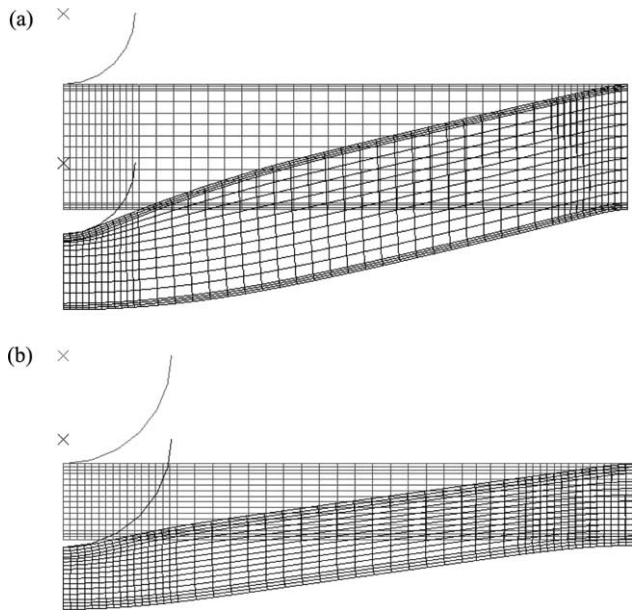

Fig. 10. Deformed and undeformed meshes for two finite element simulations of three-point bending of clamped beams. (a) Specimen in the indentation regime (geometry no. 1), (b) specimen in the core shear regime (geometry no. 4).

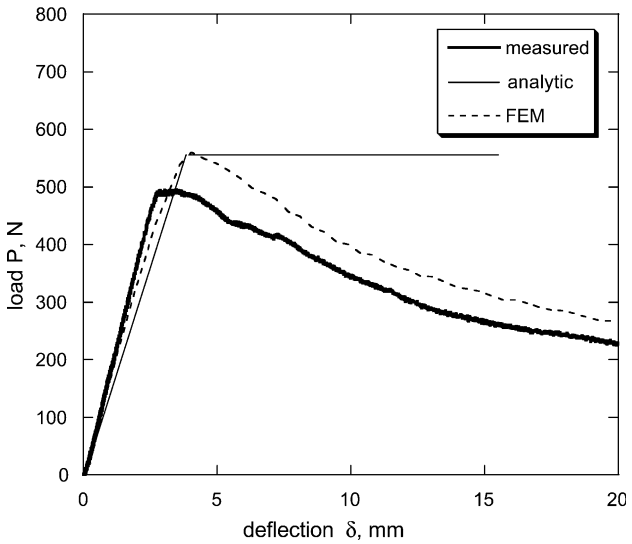

Fig. 11. Comparison between the measured, FE and analytical predictions of the load versus deflection response of a simply supported beam ($l = 200$ mm, $c = 15$ mm, $t = 0.9$ mm, geometry no. 1). The initial collapse mode of deformation was anticipated to be indentation.

FE calculation predicts the observed softening behaviour due to a progressive reduction in the beam cross-section, this post-yield behaviour is not captured by the simple analytical model. Similarly, FE and analytical predictions for the stiffness and peak load of the simply supported beam of geometry no. 4 are in reasonable agreement with the measurements, see Fig. 12. This beam collapses predominantly by core shear, and the FE simulations capture the softening due to indentation of the core. However, the FE model does not capture the sudden drop in load at $\delta \approx 8$ mm due to the microbuckling of the upper face sheet: no such failure criterion is included in the model.

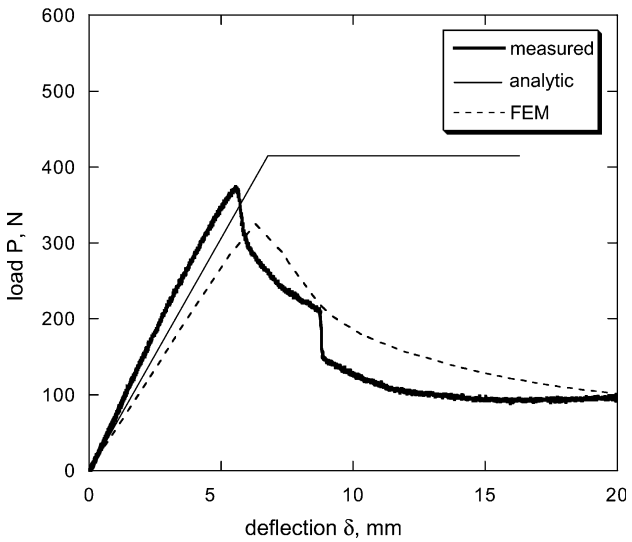

Fig. 12. Comparison between the measured, FE and analytical predictions of the load versus deflection response of a simply supported beam ($l = 150$ mm, $c = 5$ mm, $t = 0.9$ mm, geometry no. 4). The initial collapse mode of deformation was anticipated to be core shear.

Second, consider the case of clamped beams. The load versus deflection response of beam no. 1, with expected initial collapse mode of indentation, and of beam no. 4, with expected initial collapse mode of core shear are shown in Figs. 16 and 17, respectively. Excellent agreement between the measured and FE predictions is evident. On the other hand, there are some discrepancies between the analytical predictions and the measured load versus deflection response: while the simple models developed in Section 2 give very good predictions for the stiffness and the initial collapse loads of the clamped beams, they do not capture the transition from the bending-dominated response to stretching dominated behaviour, and underestimate the load carrying capacity in this transition phase. Thus, the Eqs. (2.36) and (2.39) predict the load carrying capacity and energy absorption of the beams more accurately for sandwich beams made from more ductile face sheets: in such cases the transition regime which is not captured accurately has a only a minor influence. The clamped beam test shown in Fig. 13 was terminated due to slip of the beam at the supports, but FE simulations confirmed that Eq. (2.36) accurately captures the load versus deflection response at large deformation. The beam test shown in Fig. 14 resulted in tensile failure of the front face sheet at a deflection $\delta = 17.2$ mm. This deflection is in excellent agreement with the prediction of $\delta_f = 16.7$ mm from Eq. (2.37), confirming that the analytical model is accurate at large deflections.

The measured and predicted values of the initial collapse load index $\bar{P}$ for the clamped beams are plotted in Fig. 15 as a function of the non-dimensional core thickness $\bar{c}$, for specimens lying in the indentation regime ($\bar{t} = 0.057$) and in the core shear regime ($\bar{t} = 0.17$). In this plot, the collapse load was taken to be the elastic limit of the clamped beam (i.e. equal to the load at the 'knee' in the initial portion of the load versus deflection response). The analytical model predicts that the structural load increases with $\bar{c}$ in both cases and is in good agreement with both the experiments and FE simulations.

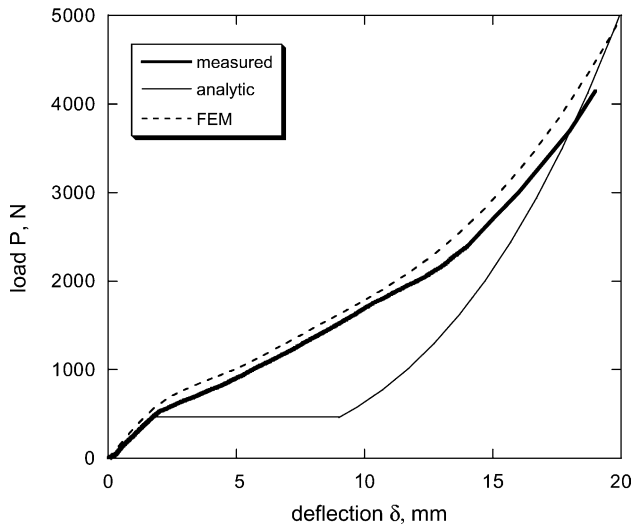

Fig. 13. Comparison between the measured, FE and analytical predictions of the load versus deflection response of a clamped beam ($l = 200$ mm, $c = 15$ mm, $t = 0.9$ mm, geometry no. 1). The initial collapse mode of deformation was anticipated to be indentation.

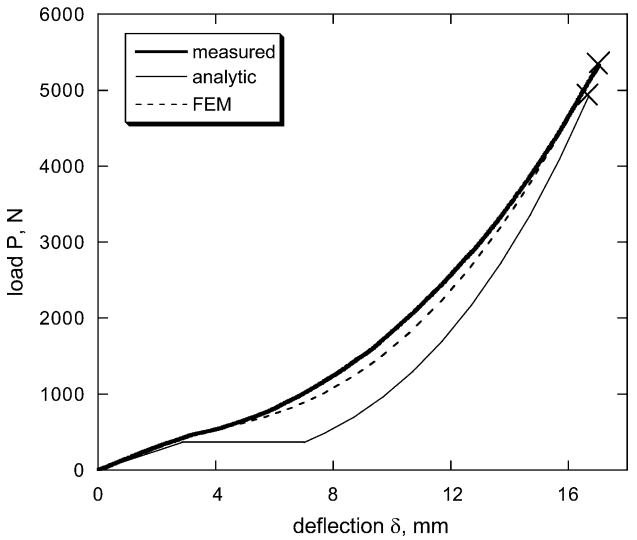

Fig. 14. Comparison between the measured, FE and analytical predictions of the load versus deflection response of a clamped beam ($l = 150$ mm, $c = 5$ mm, $t = 0.9$ mm, geometry no. 4). The initial collapse mode of deformation was anticipated to be core shear.

6. Minimum weight design

Sandwich beams can be optimised to minimise the mass against design constraints such as the initial collapse load or beam stiffness. Such a task has been undertaken for simply supported composite sandwich beams by Steeves and Fleck [3]. Here we design the geometry of a clamped sandwich beam in three-point bending to achieve minimum mass

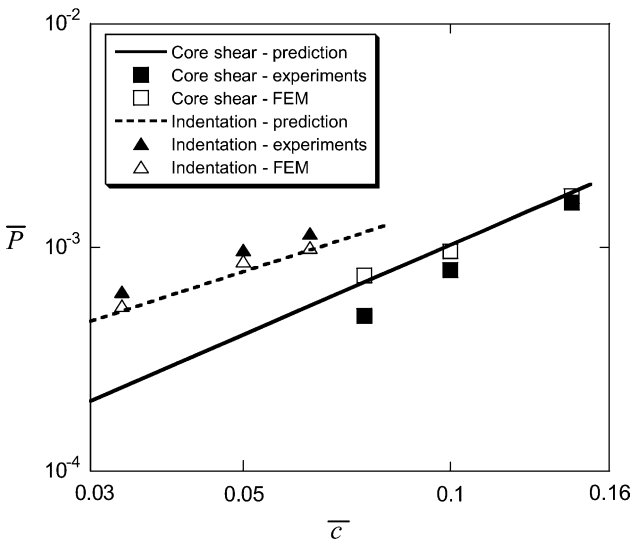

Fig. 15. Comparison between the measured, FE and analytical predictions of the non-dimensional initial collapse load $\bar{P}$ for clamped beams collapsing by indentation or core shear.

against the constraint of a prescribed initial collapse load or energy absorption.

6.1. Minimum mass design of sandwich beam for a given initial collapse load

Given a set of material properties, the optimal design is obtained by selecting the geometries $(\bar{t}, \bar{c})$ which minimise the mass $\bar{M}$ for a given initial collapse load $\bar{P}$. We introduce the non-dimensional mass index as

$$\bar{M} = \frac{M}{bl^2\rho_f} = \bar{c}(2\bar{t} + \bar{\rho}), \tag{6.1}$$

where M is the mass of the beam, ρ_f is the density of the face sheet material, ρ_c is the core density and $\bar{\rho}$ equals ρ_c/ρ_f. To help with the optimisation it is instructive to construct a collapse mechanism map for the clamped beams and to include contours of the non-dimensional collapse load $\bar{P}$ and mass $\bar{M}$, as shown in Fig. 16 for the case of sandwich beams with woven glass face sheets and the H100 PVC foam core. Both $\bar{P}$ and $\bar{M}$ increase along the leading diagonal of the map. The arrows in Fig. 16 designate the path of minimum mass with increasing $\bar{P}$, found by a numerical search method. Some portions of the path lie along the boundaries between the regions of dominance of the collapse mechanisms, others lie within these regions. Explicit expressions can be found, for the relation between $\bar{M}_{\min}$ and $\bar{P}$ along the boundaries by combining the appropriate collapse load expressions. For the portions of the minimum mass trajectory which lie within a collapse mechanism region, we can observe that $\bar{M}_{\min}$ is minimised at constant $\bar{P}$ when $\nabla\bar{M}$ is parallel to $\nabla\bar{P}$. Thus, a piecewise analytical definition of the trajectory of the minimum mass $\bar{M}_{\min}$ is given by:

(i) A horizontal line in the face microbuckling regime where

$$\bar{M}_{\min} = \left(\frac{\bar{\rho}}{2}(2-\bar{\rho})\bar{P}\right)^{1/2}. \tag{6.2}$$

(ii) a curve along the indentation/face microbuckling regime boundary with

$$\bar{M}_{\min} = \frac{\pi\bar{\rho}\bar{\sigma}}{16}\sqrt{\frac{\bar{E}}{3}} + \frac{2(2-\bar{\rho})}{\pi\bar{\sigma}}\sqrt{\frac{3}{\bar{E}}}\bar{P}. \tag{6.3}$$

(iii) a horizontal line in the indentation region, with

$$\bar{M}_{\min} = 4\left(\frac{\bar{\rho}(2-\bar{\rho}^3)}{18\pi^2\bar{\sigma}^2\bar{E}}\right)^{1/4}\bar{P}^{3/4}. \tag{6.4}$$

and

(iv) a curve along the indentation/core shear regime boundary where

$$\bar{M}_{\min} = \left(\frac{3\bar{\tau}}{\pi^2\bar{\sigma}^2\bar{E}}\right)^{1/3}(2-\bar{\rho})\bar{P}^{2/3} + \frac{\bar{\rho}\bar{P}}{2\bar{\tau}}. \tag{6.5}$$

The minimum mass $\bar{M}_{\min}$ is plotted in Fig. 17 as a function of $\bar{P}$ for sandwich beams comprising woven glass face sheets and H100 Divinycell foam core.

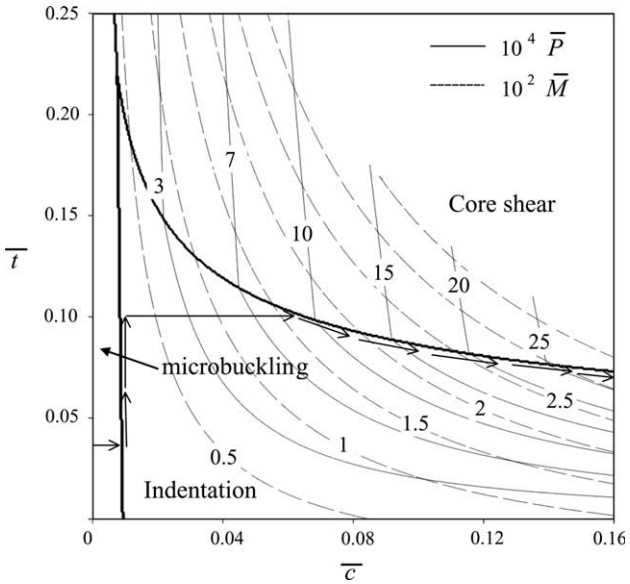

Fig. 16. Initial collapse mechanism map for clamped sandwich beams comprising woven glass–vinylester face sheets and a H100 PVC foam core ($\bar{\sigma} = 0.01$, $\bar{\tau} = 0.006$, $\bar{E} = 66.6$ and $\bar{\rho} = 0.06$). Contours of non-dimensional collapse load $\bar{P}$ and mass $\bar{M}$ are marked on this figure. The arrows indicate the trajectory of minimum mass designs for increasing $\bar{P}$.

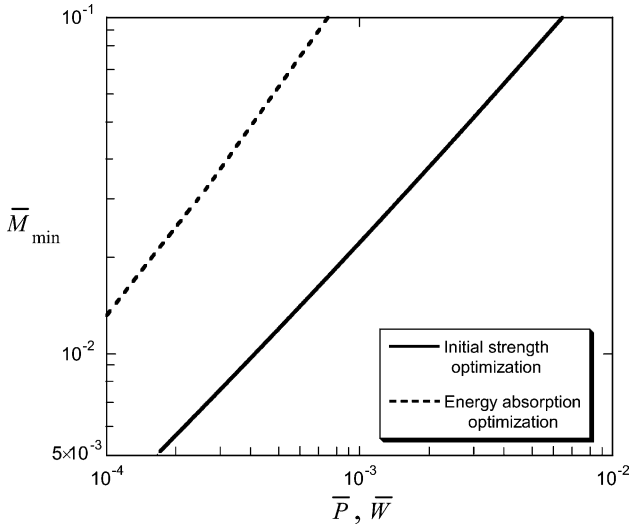

Fig. 17. Plot of the minimum mass index $\bar{M}_{\min}$ as a function of the non-dimensional initial collapse load $\bar{P}$ and of the energy absorption index $\bar{W}$, for clamped sandwich beams comprising woven glass–vinylester face sheets and a H100 PVC foam core.

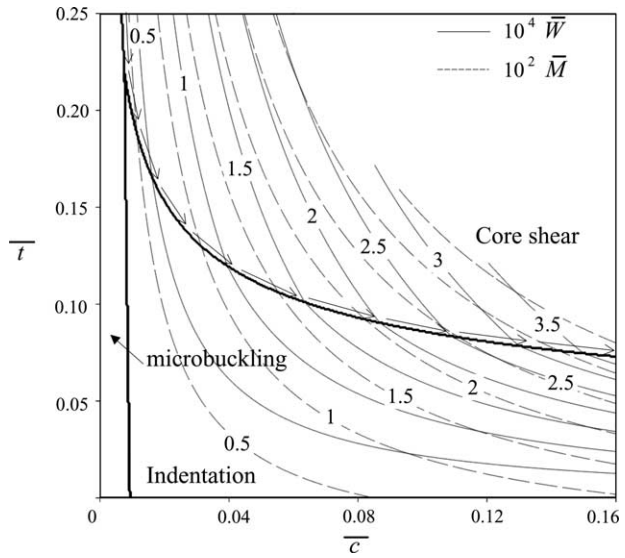

Fig. 18. Initial collapse mechanism map for clamped sandwich beams comprising woven glass–vinylester face sheets and a H100 PVC foam core ($\bar{\sigma} = 0.01$, $\bar{\tau} = 0.006$, $\bar{E} = 66.6$ and $\bar{\rho} = 0.06$). Contours of non-dimensional energy absorption $\bar{W}$ and mass $\bar{M}$ are marked on this figure. The arrows indicate the trajectory of minimum mass designs for increasing $\bar{W}$.

6.2. Optimisation with a constraint on the energy absorption capacity

Given a set of material properties, we can obtain an optimal design by selecting geometries $(\bar{t}, \bar{c})$, which minimise the mass $\bar{M}$ for a prescribed energy absorption capacity $\bar{W}$ defined as

$$\bar{W} = \frac{W}{bl^2\sigma_f}, \tag{6.6}$$

where W is given by Eq. (2.39). In Fig. 18 contours of $\bar{W}$ are plotted on the initial collapse mechanism map along with contours of $\bar{M}$, for sandwich beams comprising woven glass face sheet and the H100 Divinycell foam core. The arrows in Fig. 18 designate the path of minimum mass with increasing $\bar{W}$, obtained numerically; the corresponding minimum mass $\bar{M}_{\min}$ is plotted in Fig. 17 as a function of $\bar{W}$. It is worth noting that for high values of $\bar{P}$ and $\bar{W}$, the optimal geometries lie along the boundaries of the core shear and indentation regimes of the initial collapse mechanism map.

7. Concluding remarks

This study explores the effect of simply supported and clamped boundary conditions upon the load versus deflection response of composite sandwich beams. First, analytical formulae are presented for the stiffness and initial collapse loads. Face microbuckling, core shear and indentation are the competing initial collapse mechanisms for both boundary conditions.

Sandwich beams comprising woven glass–vinylester face sheets and a PVC foam core have been tested in three-point bending with simply supported and clamped boundary conditions. Such beams are commonly used in many marine applications. The simply supported beams display a peak load corresponding to the initial collapse mechanism while the clamped beams have a hardening post-yield response due to membrane stretching of the face sheets; a final loss in the load carrying capacity of clamped beams is due to tensile tearing of the upper face sheet. Analytical and FE predictions are in good agreement with the experimental measurements. The analytical formulae developed for the collapse load and energy absorption capacity of clamped beams are used to design sandwich beams that minimise the mass for either a given initial collapse load or a given energy absorption capacity. These designs serve to act as guidelines for designing sandwich beams comprising woven glass face sheets and a PVC foam core.

Acknowledgements

This work was supported by the US Office of Naval Research, contract No. 0014-91-J-1916 (monitor Dr Y.D.S. Rajapakse). The authors are grateful for helpful discussions with Dr C.A. Steeves.

References

[1] Ashby MF, Evans AG, Fleck NA, Gibson LJ, Hutchinson JW, Wadley HNC. Metal foam: a design guide. London: Butterworth/Heinemann; 2000.
[2] Zenkert D. An introduction to sandwich construction. EMAS; 1995.
[3] Steeves CA, Fleck NA. Minimum weight design for the strength of sandwich panels with composite face-sheets and a polymer foam core. Submitted to Int. J. Mech. Sci. (2004).
[4] Steeves CA, Fleck NA. Collapse of sandwich beams with composite face-sheets and a polymer foam core: experiment versus theory. Submitted to Int. J. Mech. Sci. (2004).
[5] Allen HG. Analysis and design of structural sandwich panels. New York: Pergamon Press; 1969.
[6] Deshpande VS, Fleck NA. Multiaxial yield behaviour in polymer foams. Acta Mater 2001;49(10):1859–66.
[7] Chen C, Fleck NA. A creep model for polymeric foams. Technical report 2000, CUED/C-MICROMECH/TR.32, Cambridge Centre for Micromechanics, University of Cambridge.